



City Research Online

City, University of London Institutional Repository

Citation: Reyes-Aldasoro, C. C., Björndahl, M. A., Kanthou, C. & Tozer, G. M. (2017). Topological analysis of the vasculature of angiopoietin-expressing tumours through scale-space tracing. *Communications in Computer and Information Science*, 723, pp. 285-296. doi: 10.1007/978-3-319-60964-5_25

This is the accepted version of the paper.

This version of the publication may differ from the final published version.

Permanent repository link: <https://openaccess.city.ac.uk/id/eprint/17944/>

Link to published version: https://doi.org/10.1007/978-3-319-60964-5_25

Copyright: City Research Online aims to make research outputs of City, University of London available to a wider audience. Copyright and Moral Rights remain with the author(s) and/or copyright holders. URLs from City Research Online may be freely distributed and linked to.

Reuse: Copies of full items can be used for personal research or study, educational, or not-for-profit purposes without prior permission or charge. Provided that the authors, title and full bibliographic details are credited, a hyperlink and/or URL is given for the original metadata page and the content is not changed in any way.

City Research Online:

<http://openaccess.city.ac.uk/>

publications@city.ac.uk

Topological Analysis of the Vasculature of Angiopoietin-Expressing Tumours through Scale-Space Tracing

Constantino Carlos Reyes-Aldasoro¹, Meit Bjorndahl², Chryso Kanthou², and Gillian M. Tozer²

¹ City, University of London, London EC1V 0HB, UK

² The University of Sheffield, Sheffield S10 2JF, UK

Abstract. This work describes the topological analysis of the vasculature of tumours. The analysis is performed with a scale-space technique, which traces the centrelines of *vessels* as *topological ridges* of the image intensities and then obtains a series of measurements, which are used to compare the vasculatures. Besides the measurements directly associated with the centrelines, the scales obtained allow the estimation of width and thus area covered with vessels.

Tumours of SW1222 human colorectal carcinoma xenografts were observed when growing in dorsal skin-fold window chambers in mice. Three variants of the tumours expressing either endogenous levels of angiopoietins (WT) or over-expressing either angiopoietin-1 (Ang-1) or angiopoietin-2 (Ang-2) were assessed with/without vascular targeted therapy. The scale-space technique was able to discriminate between the vasculatures of the three different tumour types prior to treatment. Results also suggested that over-expression of Ang-2 was associated with susceptibility of the tumour vasculature to the vascular disrupting agent, combretastatin A4 phosphate (CA4P). Substantiation of this finding would point to the potential of tumour Ang-2 expression as a predictive bio-marker for response to CA4P.

Keywords: Scale Space Analysis, Tracing of Vasculature, Vascular Disrupting Agents, CA4P, Tumour Microcirculation, Angiopoietin

1 Introduction

The process of formation of new vessels, in which capillaries sprout from existing vessels is known as *angiogenesis* [1] and, in adults, this process is restricted to relatively few situations such as the female reproductive cycle [2] and pathological processes such as growth of collaterals in response to obstructive arterial disease [3, 4], wound healing and tumour growth [5]. In the case of tumours, the new vasculature has become an attractive therapeutic target to prevent nutrients and oxygen reaching the tumour as well as preventing metastasis [6, 7].

Angiogenesis is largely driven by a series of growth factors, of which the *angiopoietin* family of proteins play a substantial role. The angiopoietins work

in concert with vascular endothelial growth factor A (VEGFA), with VEGFA stimulating formation of the initial vascular plexus and angiopoietin-1 (Ang-1) promoting vascular re-modelling, maturation and stabilisation [8]. During early phases of vascular sprouting, angiopoietin-2 (Ang-2) can act as a functional antagonist of Ang-1 that destabilises blood vessels prior to vascular sprouting or regression, although the precise functions of Ang-2 are highly context dependent [9].

The microtubule depolymerising agent, combretastatin A4 phosphate (CA4P; foscetretabulin) is currently in clinical trial (<http://www.mateon.com>) as a tumour vascular disrupting agent (VDA) that causes selective tumour blood flow shut-down, necrosis and growth retardation in solid tumours. Susceptibility of the tumour vasculature to CA4P is thought to relate to an immature vascular phenotype [7]. Therefore, we hypothesised that tumours over-expressing Ang-2 would be more susceptible to CA4P than those over-expressing Ang-1 or unmodified tumours, pointing to the potential of tumour angiopoietin expression analysis for predicting response to CA4P.

Murine dorsal skin-fold window chambers [10] provide a means to observe developing tumour blood vessels microscopically in longitudinal studies. Quantitative assessment of the angiogenesis process can be performed via analysis of the topological or chromatic characteristics of the resulting optical images [11].

In this work, we assessed the influence of angiopoietin expression in tumours through the comparison of a series of topological parameters: *number of vessels*, *length*, *width* and *relative area*. The mathematical description of the topology was obtained through a fully automatic vessel tracing algorithm [11] based on the scale-space ridge detection algorithm proposed by Lindeberg [12, 13].

2 Materials and Methods

2.1 Data sets

SW1222 human colorectal carcinoma cells, kindly supplied by Professor Barbara Pedley, University College London, UK, were transfected with angiopoietin-1 or angiopoietin-2 cDNA cloned into pcDNA3.1 mammalian expression vector or with empty pcDNA-3.1 vector alone. cDNA was kindly supplied by Professor Pam Jones, University of Leeds, UK. The resulting cells transfected with empty vector were designated wild-type (WT). Stable transfectants were selected in G418-containing medium and translation of appropriate gene products was confirmed by western blotting (data not shown). Cells over-expressing angiopoietin-1 or angiopoietin-2 were designated Ang-1 and Ang-2 respectively.

Methodological details of the animal experimentation have been described previously [14], but are included here briefly for completeness. Animal experiments were conducted in accordance with the United Kingdom Home Office Animals (Scientific Procedures) Act 1986, with local ethical approval and in line with the published Guidelines for the Welfare of Animals in Cancer Research [15]. Surgical procedures on severe-combined immune-deficient (SCID)

mice consisted of implanting an aluminium window chamber (total weight ~ 2 g), designed to hold parallel glass windows $200 \mu\text{m}$ apart to allow tumour growth, into a dorsal skin-fold under general anaesthesia. SW1222 human colorectal carcinoma cells were grown as hanging drop cultures on the lids of 60 mm plastic petri dishes inverted over dishes containing 4 ml DMEM containing standard antibiotics. Hanging drops were established from 1×10^5 SW1222 cells in $20 \mu\text{l}$ DMEM supplemented with 10% foetal calf serum and 4 mmol/l glutamine plus standard antibiotics. After 3-4 days of growth, the cell aggregates from the drops were transplanted directly onto the exposed panniculus muscle within the dorsal skin-fold window chamber preparations and the chambers closed with a glass cover-slip. Treatments and image capturing were started approximately 10-12 days after surgery.

Mice were implanted with WT, Ang-1 or Ang-2 tumour cells and, once established, were treated with either 30 mg/kg of CA4P or saline as a control, administered intraperitoneally (i.p.). CA4P was kindly supplied by Professor GR Pettit, Arizona State University, Tempe, AZ, USA.

The distribution of the mice into treatment groups was: Ang-1/CA4P ($n = 5$), Ang-1/control ($n = 6$), Ang-2/CA4P ($n = 6$), Ang-2/control ($n = 6$), WT/CA4P ($n = 4$), WT/control ($n = 2$). All tumours were observed longitudinally before (time=0) and up to 24 h (time=2.5, 15, 30, 60, 180, 360, 1440 min) after treatment.

Transmitted light images from a Nikon Eclipse E600FN microscope fitted with a $\times 2.5$ and $\times 10$ objective and incorporating illumination from a 12 V/100 W halogen light source were acquired from 29 restrained window chamber-bearing mice at 2 regions of interest (ROI) at different locations within the tumours, as illustrated in Fig. 1. In total, **four hundred and sixty four** images were acquired and processed.

The variability of the vasculatures obtained is illustrated in Fig. 2. Control tumours experienced remodelling of the vasculature within this time period, as illustrated in Fig. 3.

2.2 Scale Space Analysis

The scale-space approach [12, 13] is a multiscale technique in which a progressive low pass filtering is applied to an image with the intention of detecting features of different dimensions. The features can be of different nature, e.g. ridges, edges or blobs. Fine features will be detected at initial scales, with minimal smoothing, whilst large or coarse features will be detected with considerable smoothing of the images. Scale-space algorithms are *intensity-based* as opposed to clustering or deformable models. The details of the implementation of a scale-space vessel tracing implementation have been previously described in [11]. Essentially, the centreline of vessels was detected as a *ridge* with the intensity f of a given pixel at position (x, y) as the height in a topographical analogy. It is important to notice some limitations of the method: (a) the intensity of a physiological vessel in the image will guide the tracing process. Therefore, if a vessel does not show contrast against the tissue it may not be traced; (b) a physiological vessel may experience

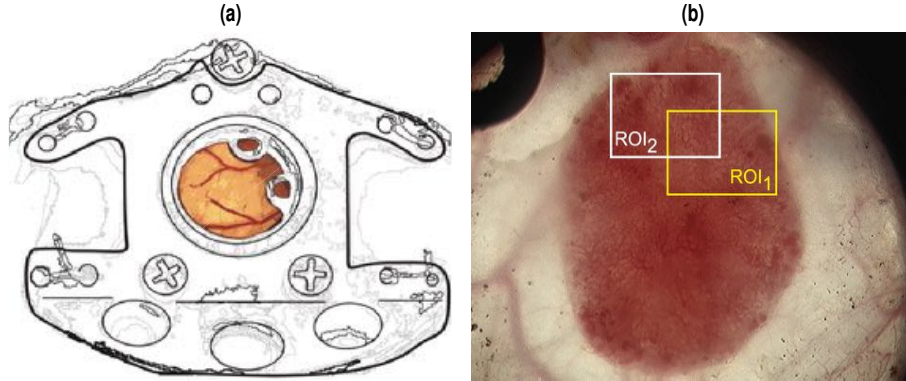


Fig. 1: (a) Illustration of a dorsal skin-fold window chamber, which is implanted in the dorsal skin of a mouse and through which the vasculature of a tumour can be observed over time. (b) One representative image acquired with a $\times 2.5$ microscope objective. The size of the regions of interest to be captured with a $\times 10$ microscope objective is illustrated with white and yellow boxes.

changes of intensity within its centreline and in some cases a single vessel may appear as two segments or traced vessels; (c) crossings of vessels may imply discontinuity of the tracing. Thus, the measurement of *number of vessels* should be considered as an approximation and may differ from a manually obtained measurement.

The scale-space representation of a function $f(x, y)$ can be defined as the convolution with a Gaussian $g(x, y; t)$ where t corresponds to the width of a Gaussian:

$$L(x, y; t) = g(x, y; t) * f(x, y) = \frac{1}{(2\pi t)} e^{-\frac{(x^2+y^2)}{(2t)}} * f(x, y) \quad (1)$$

Then, the Hessian Matrix can be formed with the normalised first and second derivatives in x and y dimensions (Lx, Lxx, Ly, Lyy).

$$H = \begin{bmatrix} \partial_x \partial_x f & \partial_y \partial_x f \\ \partial_x \partial_y f & \partial_y \partial_y f \end{bmatrix} = \begin{bmatrix} L_{xx} & L_{yx} \\ L_{xy} & L_{yy} \end{bmatrix} \quad (2)$$

Regions of maxima and minima in H were calculated when the derivatives reached zero. To obtain the centrelines of vessels, or ridges in a topological analogy, it was necessary to convert from the (x, y) coordinate system to a local (p, q) system aligned with the eigendirections of H :

$$\begin{aligned} L_p &= \partial p L = (\sin\beta \partial_x - \cos\beta \partial_y) L, \\ L_q &= \partial q L = (\cos\beta \partial_x + \sin\beta \partial_y) L, \\ L_{pq} &= \partial p \partial q L = (\cos\beta \partial_x + \sin\beta \partial_y) (\sin\beta \partial_x - \cos\beta \partial_y) L, \end{aligned} \quad (3)$$

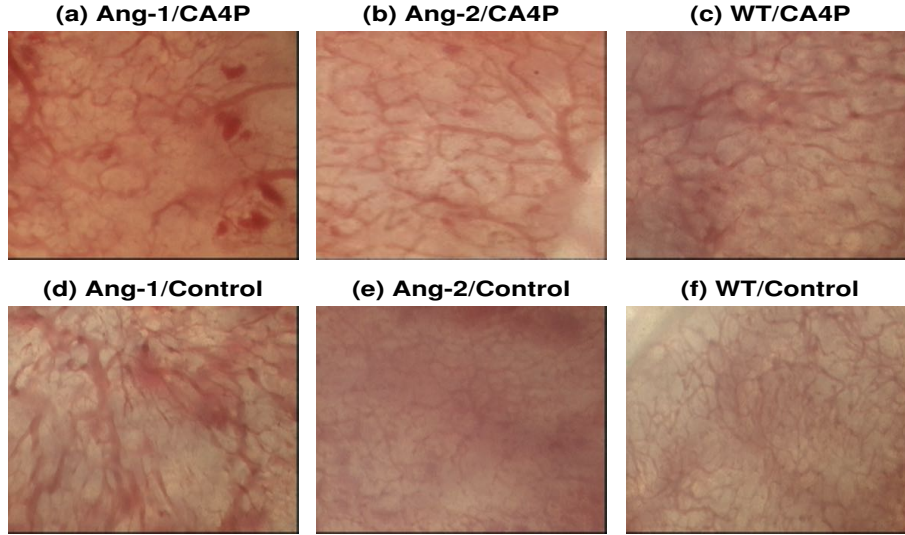


Fig. 2: ROIs from tumours within different treatment groups showing representative vasculatures. Notice the variability of vasculature in terms of size, density, colour, etc.

where β denotes the angle of rotation of the coordinate system and it was defined by:

$$\begin{aligned} \cos\beta \Big|_{(x_0, y_0)} &= \sqrt{\frac{1}{2} \left(1 + \frac{L_{xx} - L_{yy}}{(L_{xx} - L_{yy})^2 + 4L_{xy}^2} \right)} \Big|_{(x_0, y_0)}, \\ \sin\beta \Big|_{(x_0, y_0)} &= (\text{sign}(L_{xy})) \times \sqrt{\frac{1}{2} \left(1 - \frac{L_{xx} - L_{yy}}{(L_{xx} - L_{yy})^2 + 4L_{xy}^2} \right)} \Big|_{(x_0, y_0)}. \end{aligned} \quad (4)$$

The ridges at different scales constituted a scale-space ridge surface and were defined as the points of $(L_p, L_{pp}, L_q, L_{qq})$ that fulfilled the conditions of maxima at every scale. L, L_x, L_y, L_{pp} , and L_{qq} are illustrated in Fig. 4 for three scales. Finally, a *scale-space ridge* was simplified from the ridge surface by selecting the points where the surface had maximal values by a given norm. Thus, fine ridges were detected at fine scales, whilst coarse ridges had higher norm values at larger scales. A scale-space *vessel* was subsequently defined as an individual ridge detected by the algorithm, noticing that the changes of intensity may break a physical vessel into two or more *vessels*.

A large number of measurements can be obtained from the traced vessels, but for this work we concentrated on the following: number of vessels, average vessel length, average vessel diameter, and relative area of the ROI covered by vessels. The *length* and *number* are direct measurements. The *diameter* is estimated as proportional to the scale where the ridge was selected. The *area* is derived from the combination of diameter and the length of each traced vessel. The *relative*

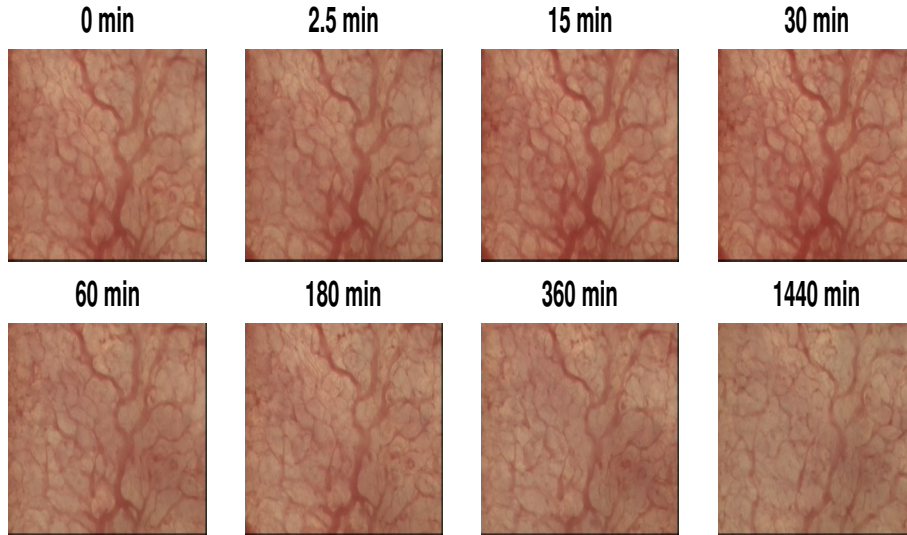


Fig. 3: Longitudinal acquisition of one tumour. Notice the variation of the thickness and position of the vasculature.

area is the ratio of the area previously calculated over the total area of the tumour tissue in the ROI. In addition, it is possible to rank the vessels by their *saliency*, i.e. the contrast between the vessel itself and the surrounding regions, in order to distinguish the top 5, 10, 50, etc. vessels. Fig. 5 illustrates results of length, diameter, area and saliency for two time points of the tumour of Fig. 3.

All algorithms were implemented in MATLAB[®] (The Mathworks[™], Natick, USA). Statistical tests of one-way Analysis of Variance (ANOVA) followed by a Tukey post-test to compare individual groups were performed in MATLAB and GraphPad Prism v7.0b.

3 Results and Discussion

The 464 images described in section 2.1 were traced with the scale-space algorithm previously described. The following measurements were selected for analysis: *number of vessels*, *average diameter*, *average length* and *relative area covered by the vessels*. Each of these measurements was calculated for the three different tumour types (*Ang-1*, *Ang-2*, *WT*), two ROIs (*1*, *2*), treated or control (*CA4P*, *control*) and eight time points (*1 - 8*). Data from the two ROIs were pooled for each tumour.

Results for the three tumour types at time $t = 0$, that is before treatment was administered, are shown in Fig. 6. p -values for a one-way ANOVA test with a Tukey post-test are presented within the figure. Boxplot whiskers indicate minimum and maximum values, and the box is formed by lines at the median, first and third quartiles.

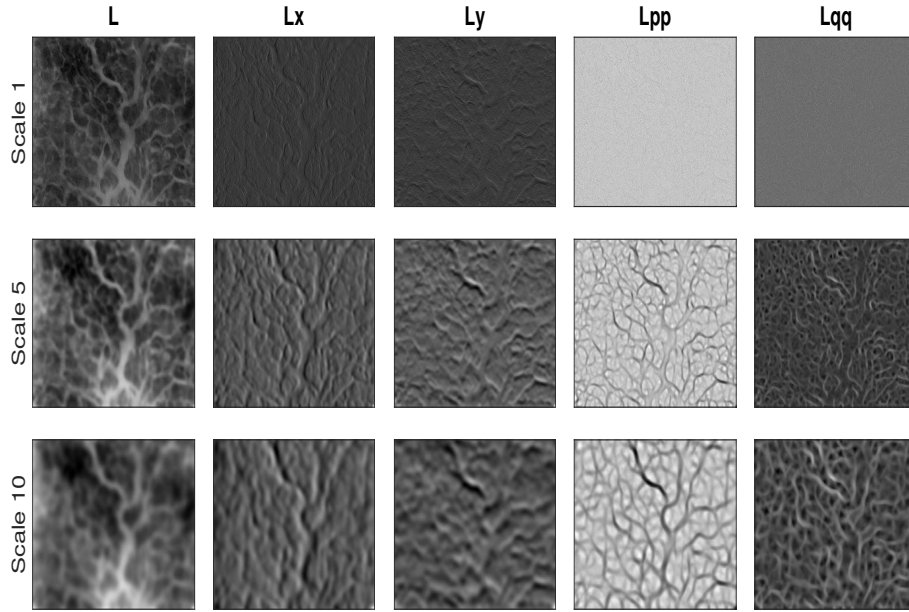


Fig. 4: Illustration of a Scale-Space process where the intensity of an image is filtered at different scales (vertical) and derivatives in different directions highlight features at each scale.

Ang-1 tumours displayed higher average length, diameter and relative area of blood vessels compared with Ang-2 tumours (Fig. 6). Furthermore, the relative area measurement was significantly lower for Ang-2 tumours than either Ang-1 tumours or WT tumours. Ang-1 expression has previously been associated with development of wide vessels, consistent with these findings [9]. Ang-2 can act as an antagonist for Ang-1, causing vessel destabilisation [16–21], which may also have contributed to our results. Interestingly, angiopoietin over-expression did not influence the number of vessels identified by the algorithm (Fig. 6(a)), suggesting that effects were confined to the diameter and length and not the number of traced vessels.

Figures 7, 8, 9 and 10 show the effects of CA4P treatment versus control over time on the four vascular parameters shown in Fig 6, for each of the three tumour types. The number of vessels remained relatively stable in each of the tumour types over time, whether treated with CA4P or not. However, CA4P appeared to reduce average diameter and length of blood vessels in all tumour types within 3 h of treatment (Figs. 7 and 8), leading to a similar effect on vascular area (Fig. 10). This confirms the rapid response of tumour vasculature to CA4P reported in other tumour types (e.g. [22]). In general, Ang-2 tumours were most affected by CA4P, although further work, including functional assays, would be needed to determine whether differences in response are statistically significant.

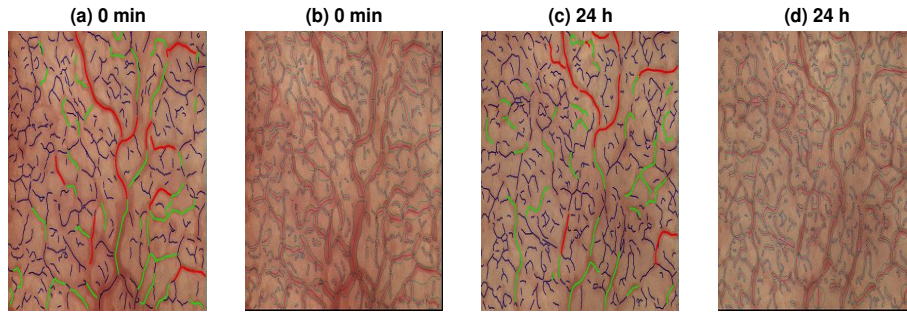


Fig. 5: (a,c) Traced vessels overlaid on two time points from a single tumour. The vessels have been ranked and the top 10 are traced in red, 11-50 are traced in light green and the rest in thinner black lines. Notice the changes of the vascular topology over time. (b,d) Traced vessels and the inferred thickness of each vessel denoted by dark shading. The relative area covered was obtained by the ratio of the shaded pixels over the total area of the image.

4 Conclusions

The scale-space algorithm here described was an effective technique to analyse the topological variation of the vasculature of three different tumour types. Besides the vascular parameters analysed here, it would be possible to extract other parameters such as total length of the vasculature, length of longest vessels and branching patterns or other non-geometrical measurements such as saturation or hue.

The results presented here are consistent with Ang-1 acting as a stabilising influence in angiogenesis and Ang-2 having antagonistic properties. However, further analysis is required as the effects of Ang-2 have been reported to have opposing effects under different circumstances such as in the presence of VEGFA [17, 23] or in the lymph versus blood vessel networks [24]. The well known tumour vascular disrupting effect of CA4P was confirmed in the current study and there was a suggestion that tumour cell over-expression of Ang-2 resulted in an increased response to CA4P. If this is substantiated in further studies, it would confirm our hypothesis and point to the potential of tumour angiopoietin expression analysis for aiding the development of predictive biomarkers of response to CA4P.

5 Code

The code and a brief user manual is freely available as Matlab functions from the author's website:

<http://www.staff.city.ac.uk/~sbbk034/tracingD.php?idMem=software>

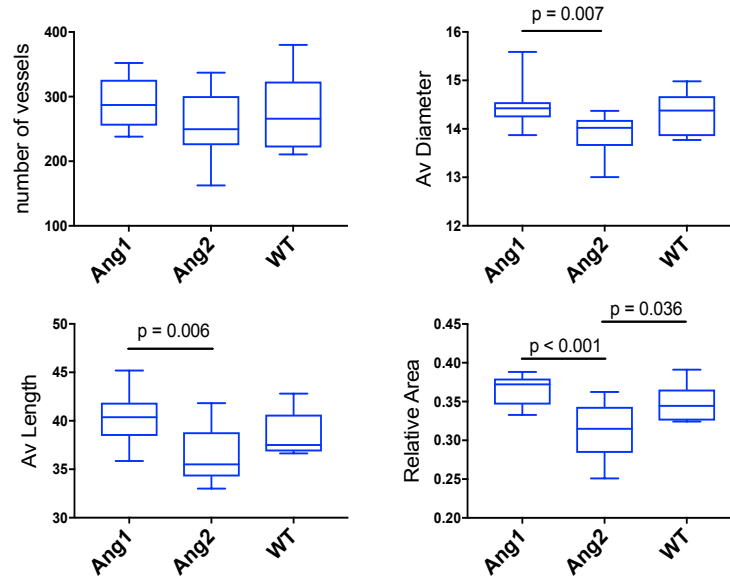


Fig. 6: Boxplots summarising the statistical difference between the three tumour types at time $t = 0$, before the start of treatment. The p – values for 1-way ANOVA followed by a Tukey post-test are included within the figures. There was a statistical difference between Ang-1 and Ang-2 for the diameter, length and relative areas, and between Ang-2 and WT for relative area only.

6 Acknowledgements

We thank Professor Barbara Pedley for her gift of the SW1222 tumour cell line and Professor Pam Jones for her gift of Ang-1 and Ang-2 cDNA. We thank Drs Olga Greco and Sheila Harris for their contributions to development of the genetically modified cell lines. We thank staff at the University of Sheffield for their care of the animals used in this study. This work was funded by Programme Grant C1276/A9993 from Cancer Research UK.

References

1. Risau, W.: Differentiation of endothelium. *FASEB J.* 9(10), 926–933 (1995)
2. Jiang, Y.F., Hsu, M.C., Cheng, C.H., Tsui, K.H., Chiu, C.H.: Ultrastructural changes of goat corpus luteum during the estrous cycle. *Animal Reproduction Science* 170, 38–50 (2016)
3. Zhang, H., van Olden, C., Sweeney, D., Martin-Rendon, E.: Blood vessel repair and regeneration in the ischaemic heart. *Open Heart* 1(1), e000016 (2014), <http://openheart.bmj.com/content/1/1/e000016>

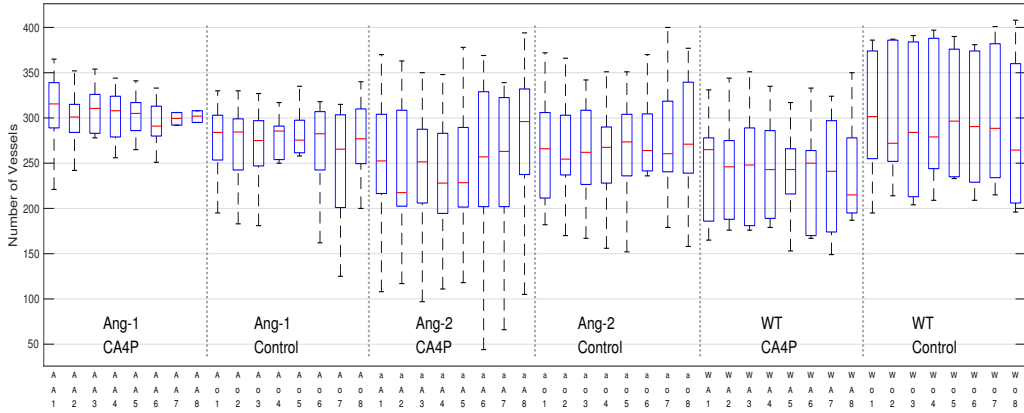


Fig. 7: Boxplots of the Number of Vessels as determined by the tumour type Ang-1, Ang-2 and WT (A/a/W), treatment for CA4P or control (A/o) and the time of acquisition (1-8).

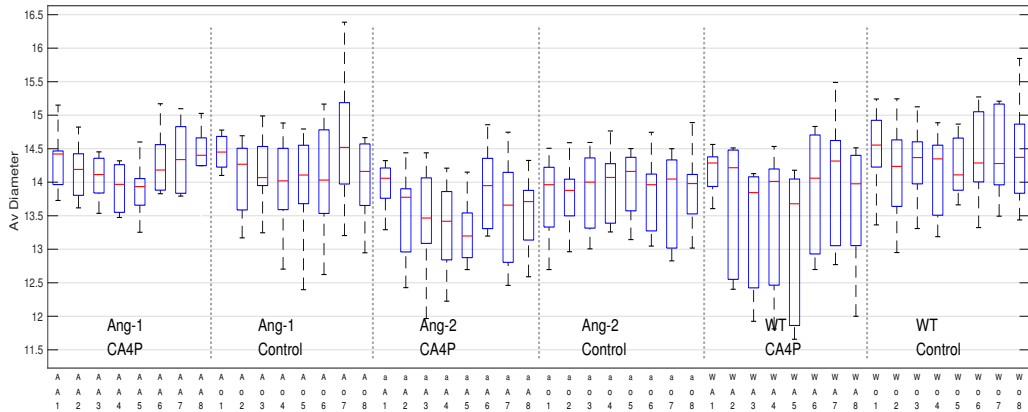


Fig. 8: Boxplots of the Diameter [pixels] as determined by the tumour type Ang-1, Ang-2 and WT (A/a/W), treatment for CA4P or control (A/o) and the time of acquisition (1-8).

4. Collinson, D., Donnelly, R.: Therapeutic angiogenesis in peripheral arterial disease: Can biotechnology produce an effective collateral circulation? *Eur J Vascular Endovascular Surgery* 28(1), 9 – 23 (2004)
5. Hanahan, D., Folkman, J.: Patterns and emerging mechanisms of the angiogenic switch during tumorigenesis. *Cell* 86(3), 353–364 (1996)
6. Tozer, G.M., Bicknell, R.: Therapeutic targeting of the tumor vasculature. *Semin Radiat Oncol.* 14(3), 222–232 (2004)

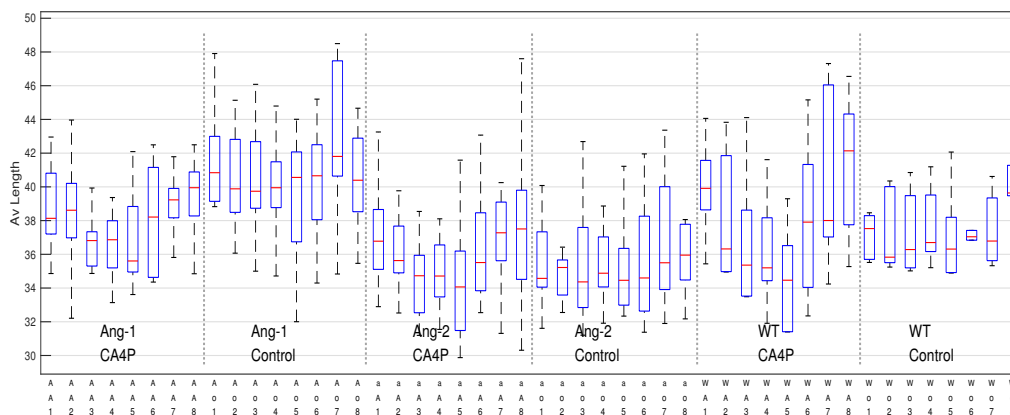


Fig. 9: Boxplots of the Length [pixels] as determined by the tumour type Ang-1, Ang-2 and WT (A/a/W), treatment for CA4P or control (A/o) and the time of acquisition (1-8).

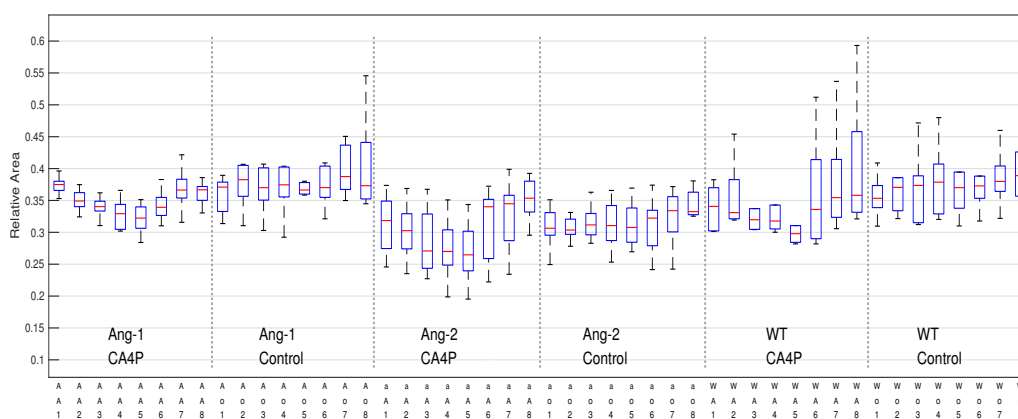


Fig. 10: Boxplots of the Relative Area as determined by the tumour type Ang-1, Ang-2 and WT (A/a/W), treatment for CA4P or control (A/o) and the time of acquisition (1-8).

7. Tozer, G.M., Kanthou, C., Baguley, B.C.: Disrupting tumour blood vessels. *Nat Rev Cancer* 5(6), 423–435 (2005)
8. Augustin, H., Koh, G., Thurston, G., Alitalo, K.: Control of vascular morphogenesis and homeostasis through the angiopoietin-tie system. *Nat Rev Mol Cell Biol.* 10(3), 165–77 (2009)
9. Thurston, G., Daly, C.: The Complex Role of Angiopoietin-2 in the AngiopoietinTie Signaling Pathway. *Cold Spring Harbor Perspectives in Medicine* 2(9), a006650 (2012), <http://perspectivesinmedicine.cshlp.org/content/2/9/a006650>

10. Koehl, G.E., Gaumann, A., Geissler, E.K.: Intravital microscopy of tumor angiogenesis and regression in the dorsal skin fold chamber: mechanistic insights and preclinical testing of therapeutic strategies. *Clin. Exp. Metastasis* 264, 329–344 (2009)
11. Reyes-Aldasoro, C.C., Bjorndahl, M.A., Akerman, S., Ibrahim, J., Griffiths, M.K., Tozer, G.M.: Online chromatic and scale-space microvessel-tracing analysis for transmitted light optical images. *Microvasc Res.* 84(3), 330–339 (2012)
12. Lindeberg, T.: Feature detection with automatic scale selection. *Int J Comp Vision* 30(2), 79–116 (1998)
13. Lindeberg, T.: Edge detection and ridge detection with automatic scale selection. *Int J Comp Vision* 30(2), 117–154 (1998)
14. Tozer, G.M., Ameer-Beg, S.M., Baker, J., Barber, P.R., Hill, S.A., Hodgkiss, R.J., Locke, R., Prise, V.E., Wilson, I., Vojnovic, B.: Intravital imaging of tumour vascular networks using multi-photon fluorescence microscopy. *Adv Drug Deliv Rev.* 57(1), 135–152 (2005)
15. Workman, P., Aboagye, E.O., Balkwill, F., Balmain, A., Bruder, G., Chaplin, D.J., Double, J.A., Everitt, J., Farningham, D.A.H., Glennie, M.J., Kelland, L.R., Robinson, V., Stratford, I.J., Tozer, G.M., Watson, S., Wedge, S.R., Eccles, S.A., Committee of the National Cancer Research Institute: Guidelines for the welfare and use of animals in cancer research. *Brit J Cancer* 102(11), 1555–1577 (2010)
16. Zagzag, D., Hooper, A., Friedlander, D.R., Chan, W., Holash, J., Wiegand, S.J., Yancopoulos, G.D., Grumet, M.: In situ expression of angiopoietins in astrocytomas identifies angiopoietin-2 as an early marker of tumor angiogenesis. *Exp Neurol.* 159(2), 391–400 (1999)
17. Plank, M., Sleeman, B., Jones, P.: The role of the angiopoietins in tumour angiogenesis. *Growth Factors* 22(1), 1–11 (2004)
18. Maisonpierre, P.C., Suri, C., Jones, P.F., Bartunkova, S., Wiegand, S.J., Radziejewski, C., Compton, D., McClain, J., Aldrich, T.H., Papadopoulos, N., Daly, T.J., Davis, S., Sato, T.N., Yancopoulos, G.D.: Angiopoietin-2, a natural antagonist for Tie2 that disrupts in vivo angiogenesis. *Science* 277, 55–60 (1997)
19. Hanahan, D.: Signaling vascular morphogenesis and maintenance. *Science* 277(5322), 48–50 (1997)
20. Holash, J., Maisonpierre, P.C., Compton, D., Boland, P., Alexander, C.R., Zagzag, D., Yancopoulos, G.D., Wiegand, S.J.: Vessel cooption, regression, and growth in tumors mediated by angiopoietins and VEGF. *Science* 284(5422), 1994–1998 (1999)
21. Koblizek, T.I., Weiss, C., Yancopoulos, G.D., Deutsch, U., Risau, W.: Angiopoietin-1 induces sprouting angiogenesis in vitro. *Curr Biol.* 8(9), 529–532 (1998)
22. Tozer, G.M., Prise, V.E., Wilson, J., Cemazar, M., Shan, S., Dewhirst, M.W., Barber, P.R., Vojnovic, B., Chaplin, D.J.: Mechanisms associated with tumor vascular shut-down induced by combretastatin A-4 phosphate: intravital microscopy and measurement of vascular permeability. *Cancer Res.* 61(17), 6413–6422 (2001)
23. Hata, K., Nakayama, K., Fujiwaki, R., Katabuchi, H., Okamura, H., Miyazaki, K.: Expression of the angiopoietin-1, angiopoietin-2, Tie2, and vascular endothelial growth factor gene in epithelial ovarian cancer. *Gynecol Oncol.* 93(1), 215–222 (2004)
24. Gale, N.W., Thurston, G., Hackett, S.F., Renard, R., Wang, Q., McClain, J., Martin, C., Witte, C., Witte, M.H., Jackson, D., Suri, C., Campochiaro, P.A., Wiegand, S.J., Yancopoulos, G.D.: Angiopoietin-2 is required for postnatal angiogenesis and lymphatic patterning, and only the latter role is rescued by Angiopoietin-1. *Dev Cell* 3(3), 411–423 (2002)